ISSN 2354-9114 (online), ISSN 0024-9521 (print)
Indonesian Journal of Geography Vol 56, No.2 (2024): 159-169
DOI: 10.22146/ijg.81788 website: https://jurnal.ugm.ac.id/ijg

INDONESIAN JOURNAL OF GEOGRAPHY

RESEARCH ARTICLE

Dynamics of Morphology Changes in Progo River Due to Lahar Transport from Merapi Volcano

Adib Prima Adhitama([1*]), Retnadi Heru Jatmiko([2]), Estuning Tyas Wulan Mei([3]), Junun Sartohadi([4])
([1]) The Graduate School of Universitas Gadjah Mada, Indonesia
([2]) Faculty of Geography, Universitas Gadjah Mada, Indonesia
([3]) Faculty of Geography, Universitas Gadjah Mada, Indonesia
([4]) Faculty of Agriculture, Universitas Gadjah Mada, Indonesia

Received: 2023-01-27
Revised: 2023-09-30
Accepted: 2024-06-27
Published: 2024-07-19

Key words: lahar flood; river morphology; sinuosity; Merapi; spatial-temporal analysis

Correspondent email :
adibprimaadhitama@mail.ugm.ac.id
retnadih@ugm.ac.id
estu.mei@ugm.ac.id
junun@ugm.ac.id

Abstract This study aims to comprehensively examine the dynamics of river morphology changes influenced by the occurrence of two distinct lahar floods which occurred in the years 1975 and 2010 respectively. In order to achieve the stated objectives, temporal images representing the conditions of the study area several years after the occurrence of the lahar floods were obtained and used to examine river morphology changes. Furthermore, temporal data from remote sensing and UAV were collected and used to analyze morphology changes of river valleys in the study area. The analysis was carried out using three parameters namely river slope, riverbank morphology, and river curvature. River slope was 0.74%, showing a relatively flat gradient, and this condition resulted in a meandering river morphology. Morphology of riverbank was observed to have the "U" shape, providing more surface area for river water to drain. Additionally, the sinuosity ratio (SR) during the two lahar flood periods were found to be dynamic. During the 2010 lahar flood period, the SR pre-lahar flood was 1.92, which increased significantly to 2.65 eight months after the event, and decreased drastically to 1.60 one year later. It is important to comprehend that the main factor responsible for these changes during the period was flood. The obtained results showed that the SR value for the next decade, starting from 2010, experienced consistent fluctuations. These fluctuations provided evidence that river morphology was always experiencing changes even without major triggers. For the analysis of the 1975 lahar flood period, the SR value was obtained from the PBB maps three years before the event, five years post-event, and from an analysis of Google Earth images ten years after the disaster. Similarly, the SR in this period was observed to fluctuate significantly, and the meander became simpler in the tenth year after the occurrence of flood. The results of this study provide evidence that spatial analysis with temporal images is more efficient and economical for studying the dynamics of river morphology.

1. Introduction

The 2010 Merapi eruption is one of the largest volcanic eruptions experienced in the 21st century. This was evidenced by a previous study which categorized the eruption as more explosive than previous eruptions in the present century (Saepuloh et al., 2013). Furthermore, it is important to emphasize that the eruption led to the spread of volcanic materials in various forms, such as gas, lava, ash, and lahar across the affected area. Among these materials, lahar has been observed to pose a significant danger. This material is deposited to the environment as a result of debris flows, transitional flows, or high-concentration flows from volcanoes, with the exception of normal flows ("Encyclopedia of Volcanoes," 2000). Based on observations, lahar hazards are typically influenced by four controlling factors namely rainwater boost (Asmara et al., 2021), easily entrained debris, steep slopes, and triggering mechanisms ('Encyclopedia of volcanoes', 2000; Mead, Magill, and Hilton, 2016).

According to various previous studies, lahar hazards typically occur several years after the occurrence of a volcanic eruption and cover up to tens of kilometers in range. One of the lethal characteristics of this form of hazard is that it flows far downstream (Gudmundsson, 2015; Minami et al., 2019; Thouret et al., 2020). For example, a previous investigation elucidated that during the 2010 volcanic eruption, lahar flow was directed towards the southwestern part of Merapi (De Bélizal et al., 2013), adversely affecting the area (Hadmoko et al., 2018). Subsequently, the flow extended from river located west of Merapi into Progo River, resulting in the occurrence of lahar floods in Kalibawang, Kulon Progo, and its surroundings. This observation is supported by the Google Earth images obtained during the course of the present study, as shown in Figure 1. Image A shows the conditions before lahar flood on February 21, 2010, while image B presents the conditions eight months after. Based on the observations made, it was found that lahars buried tens of hectares of rice fields with sand deposits, as showed by the yellow lines in image B (Figure 1), and was observed to be a repetition of past events, specifically the volcanic eruption that took place in the same area in 1975.

Lahar flow have been found to possess the potential to adversely affect river morphology, and this is evidenced by the fact that the event pollute water bodies with both destructive

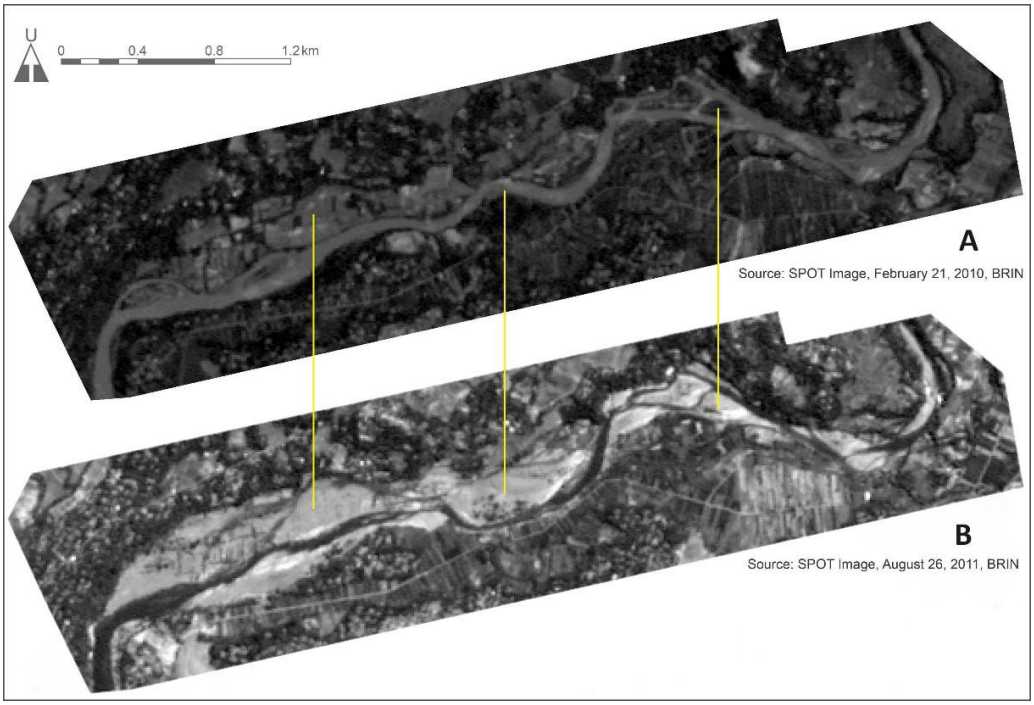

Figure 1. Comparison of conditions in the study area before and after lahar flood

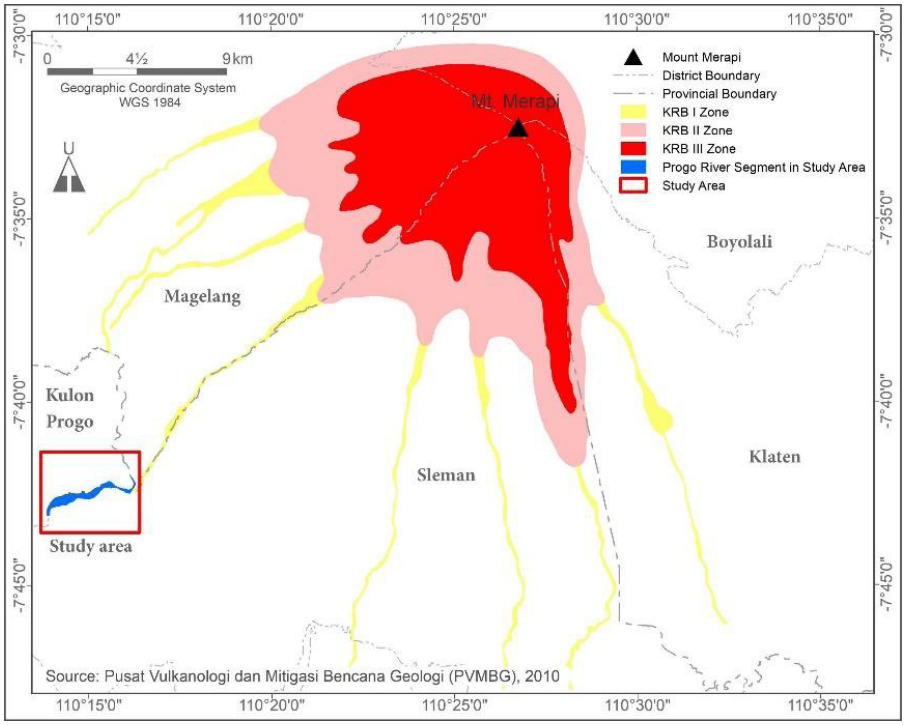

Figure 2. The 2010 KRB Map

(Saputra, 2013) and highly corrosive properties. Typically, data on past lahar events can be used as a guide for analyzing changes in river morphology (Pistolesi et al., 2014) and remote sensing data can be adopted to comprehensively examine locations that have the potential to be reflowed by streams of water (Sarif et al., 2021; Suresh et al., 2022).

Through the use of spatial analysis, this study aimed to thoroughly examine the dynamics of Progo's river morphology influenced by lahar floods, specifically in the segment of Kalibawang Sub-District, Kulon Progo. This segment is located on the southwest flank of Merapi, 30 km from Merapi cone, outside the hazard zone of the area, as shown by the 2010 Kawasan Rawan Bencana (KRB) Map (Figure 2) published by Pusat Vulkanologi dan Mitigasi Bencana Geologi (PVMBG). In this investigation, the considered elements at risk due to lahar in the observed area include human activities on agricultural and mining lands, as well as the economic value of natural resources.

This study is considered significantly important, specifically in terms of examining and analyzing the dynamics of river morphology due to massive material transport from lahar floods. Accordingly, in order to achieve the study's objectives, multi-temporal remote sensing data were collected and used to examine the annual changes in river morphology, from the pre-lahar to post-lahar periods and data processing was carried out using four distinct GIS techniques. These

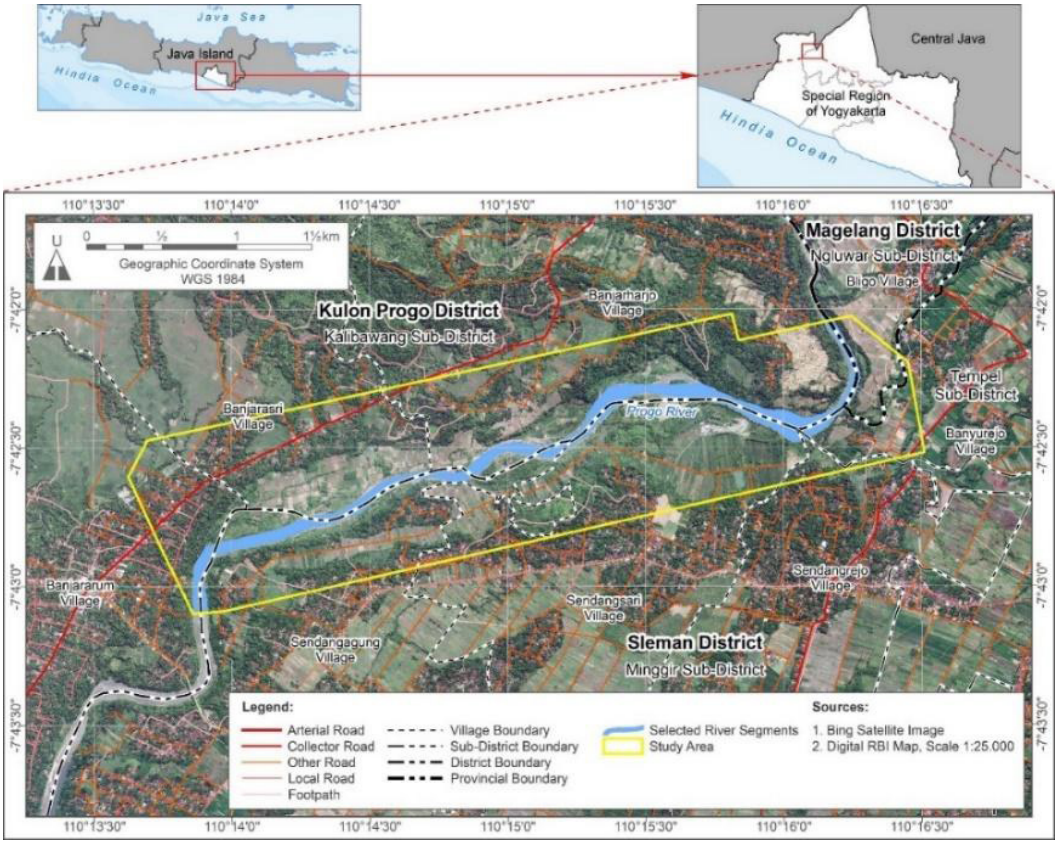

Figure 3. Map of the study area in the segment of Progo River, located in Kalibwang and Minggir Sub-District

techniques include digitization, delineation, on-screen measurements, and visual analysis. Lastly, it is anticipated that the combination of temporal imagery and GIS will make the examination of the dynamics of river morphology more efficient.

2. Methods

Study area

The study area comprises a segment of Progo River which was affected by lahar floods resulting from the volcanic eruptions of Merapi in both 1975 and 2010. This location was particularly selected because it is located outside Merapi hazard zone on the KRB Map (Figure 2), making the area an intriguing study area. Furthermore, at this location, two elements were observed to be at risk namely human activities on agricultural and mining lands, as well as the economic value of natural resource products, both of which necessitate protection (Figure 3). It is also important to comprehend that the study area is included in the administrative area of Kalibawang Sub-District, Kulon Progo District, and Minggir Sub-District, Sleman District, Yogyakarta Special Region Province. The length of the selected river segment, as shown in Figure 1, is 5,540 m and the topography of the study area is river valley surrounded by cliffs on the northern and southern parts.

Data

This study was conducted using data from temporal maps and images from various sources that represent lahar flood periods of 2010 and 1975. These two data periods were selected primarily with the aim of examining the similarities in morphology dynamic patterns after lahar floods. To achieve this objective, data from before and after floods from each period were collected and analyzed, as described in Table 1. Data for the 2010 lahar flood period comprised images from SPOT 4 Panchromatic, SPOT 6 Panchromatic and Multispectral, SPOT 7 Panchromatic and Multispectral, Google Earth, Quickbird, and mosaic orthophoto. Images of the 2010 pre-flood and post-flood periods from 2010 to 2022, with the exception of 2020, were obtained and presented. Furthermore, data for the 1975 lahar flood period constituted images from the Land and Building Tax (PBB) map of Banjarasri Village, the PBB map of Banjarharjo Village, and Google Earth. It is important to state that the dataset for this period was limited but the available data points obtained were sufficient to give a comprehensive overview of the river morphology after the event. This study also incorporated the use of a Digital Elevation Model (DEM) to examine aerial photographs obtained from Unmanned Aerial Vehicles (UAV) with the aim of measuring river slopes in the study area, which was, in turn, used to determine zones of erosion and deposition on the selected river segments. In this regard, the Aerial photos were acquired on September 12, 2022, and subsequently extracted into orthophoto mosaics for visual analysis and DEM to obtain river slope data.

Data Analysis

The parameters considered include the slope, morphology, and curvature of the observed river (Sarif et al., 2021; Suresh et al., 2022). River slope was obtained through on-screen digitation and measurements based on the UAV DEM data, while river morphology data were obtained through manual delineation of all data gathered from the 2010 and 1975 lahar flood periods. It is important to elucidate that manual delineation was carried out primarily because the technique provides certain advantages over computer-based classification (Hasan et al., 2022).

The parameter of river curvature was assessed using the sinuosity ratio, a value that shows the degree to which a river

Table 1. Various data types used in this study

Data	Years	Sources
The 2010 lahar flood		
SPOT 4 Panchromatic	2010	BRIN official data
SPOT 4 Panchromatic	2011	BRIN official data
Google Earth	2012	https://earth.google.com/web/
Google Earth	2013	https://earth.google.com/web/
Google Earth	2014	https://earth.google.com/web/
SPOT 7 Panchromatic	2015	BRIN official data
Quickbird	2016	Kementerian ATR/BPN official data
Google Earth	2017	https://earth.google.com/web/
SPOT 6 Panchromatic & Multispectral	2018	BRIN official data
Google Earth	2019	https://earth.google.com/web/
SPOT 7 Panchromatic & Multispectral	2021	BRIN official data
UAV Orthophoto	2022	Personal acquisition
The 1975 lahar flood		
PBB map of Banjarasri Village	1972	Banjarasri Village Government's official data
PBB map of Banjarharjo Village	1980	Banjarharjo Village Government official data
Google Earth	1985	https://earth.google.com/web/
DEM UAV	2022	Personal acquisition

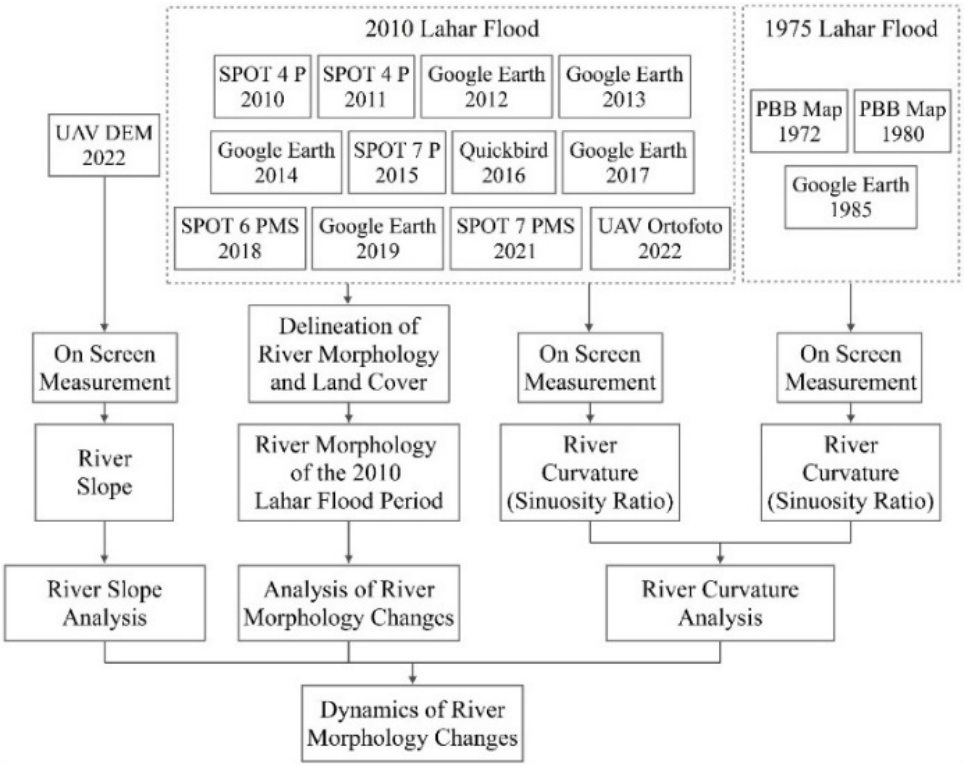

Figure 4. Study flowchart for assessing river morphology dynamics

channel is curved (Sarif et al., 2021, Charlton, 2007). This ratio is typically determined by measuring the length of a channel reached and dividing the obtained value by the straight line distance along the valley (Charlton, 2007). Generally, valley length calculation includes the distance from the upstream to the downstream of selected river segments while channel length is determined based on the centerline of each channel, including those separated by sandbars (Sarif et al., 2021). The formula used to calculate the sinuosity ratio is as follows,

$$Sinuosity\ ratio\ (SR) = \frac{Channel\ length}{Valley\ length}$$

where *Sinuosity ratio* (*SR*) represents river curvature value, C*hannel length* refers to the length of a channel reached or river segment length, and *Valley length* denotes the straight line distance along the valley. It is important to state that an SR value that is less than 1.1 shows a water body in the straight river category. However, a water body with an SR value that is between 1.1 and 1.5 is included in the sinuous river category, while an SR value greater than 1.5 shows a meandering river (Charlton, 2007). The flow of the study methods adopted during the course of this investigation is described using the flowchart presented in Figure 4.

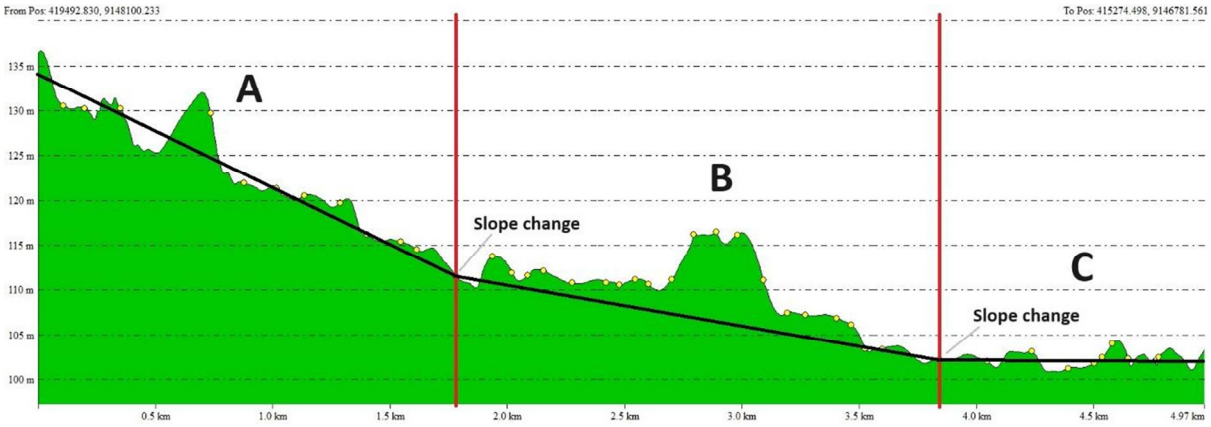

Figure 5. Longitudinal cross-section of selected river segments

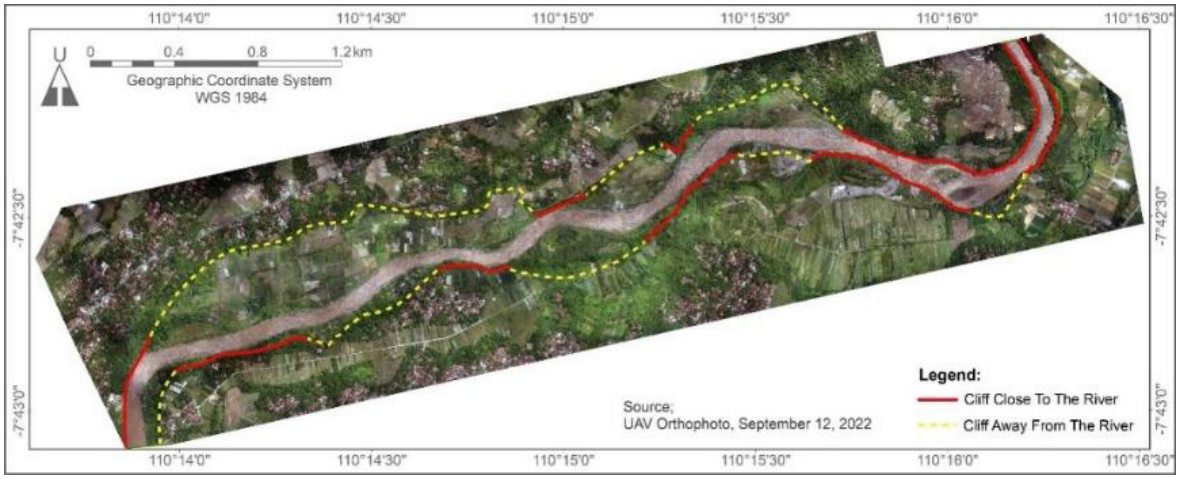

Figure 6. Position of river valley cliffs in the study area

3. Result and Discussion

River slope

In this investigation, the selected river segments had flat gradients and the longitudinal cross-section of the segments is presented in Figure 3. The height difference from upstream to downstream was observed to be 40.81 meters while the length of river segment in the study area was approximately 5,540 meters. Furthermore, the slope was 0.74, showing a relatively flat gradient (Van Zuidam, 1986), and this was further evidenced by the fact that the river possessed a meandering morphology condition. Factually, the smaller the slope, the more effective the meandering condition of a river (Charlton, 2007), and a flat topography provides more surface area for river water to drain (Suresh et al., 2022).

The slope of river from upstream to downstream was divided into three segments namely Segemrnts A, B, and C, based on the gradient, as shown in Figure 5.. The three segments were bounded by slope buckling which showed consistent changes in slope. Segments A, B, and C representing the upstream, middle, and downstream sections of the study area, were observed to have a gradient of 1.22, 0.47, and 0.14 respectively. These changes in slope show the presence of fluctuations in terms of slope morphology. The sloping side section of river is referred to as the erosion zone, while the slope transition area is the deposition zone. As a result of the erosion that took place at the erosion zone, the deposition zone became an area of sediment concentration. According to Sarif et al. (2021), river morphology typically varies primarily because rivers carry different volumes of water and sediment at different stages in response to topographical and other geomorphological conditions (Sarif et al., 2021). This statement is in accordance with the conditions in the study area, where lahar floods were observed to occur when approaching the middle to the downstream part of the study area as a result of differences in slope.

As stated in previous investigations, meandering rivers generally increase the potential for erosion, and this erosion typically occurs on the outside of the bend (Islami, 2014; Sarif et al., 2021). Each bend in river segment in the study area produced both an erosion and deposition zone, and these zones were observed to facilitate the impact of lahar flood hazards resulting from Merapi volcanic eruption. The present observation is further supported by a previous study stating that floods, particularly lahars, generally occur in areas with low slopes (Charlton, 2007).

River Morphology

One of the causes of a meandering river condition is the nature of river bank and river valley cliff morphology. In this study, the observed river possessed valley cliffs with a U-type morphology. The distance between river body and the cliffs on both sides was observed to be different across the different sections of the study area. In one section, the cliffs in the north were very close to river body while those in the south were farther away (Figure 6). Meanwhile, in the other sections, the position of the cliffs was opposite and formed a zig-zag pattern. During the course of this investigation, the position of the cliffs was considered very important for analyzing river

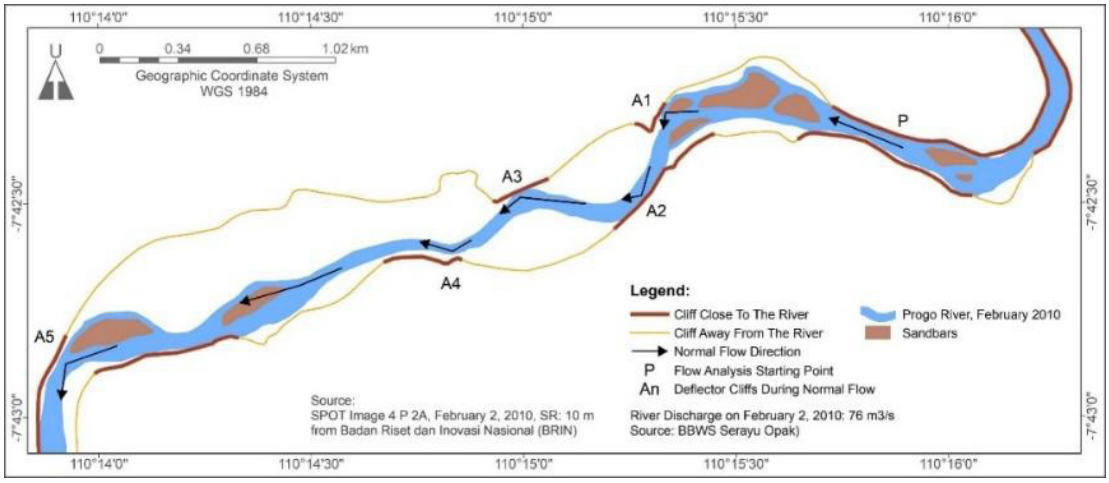

Figure 7. Flow direction before the 2010 Lahar flood

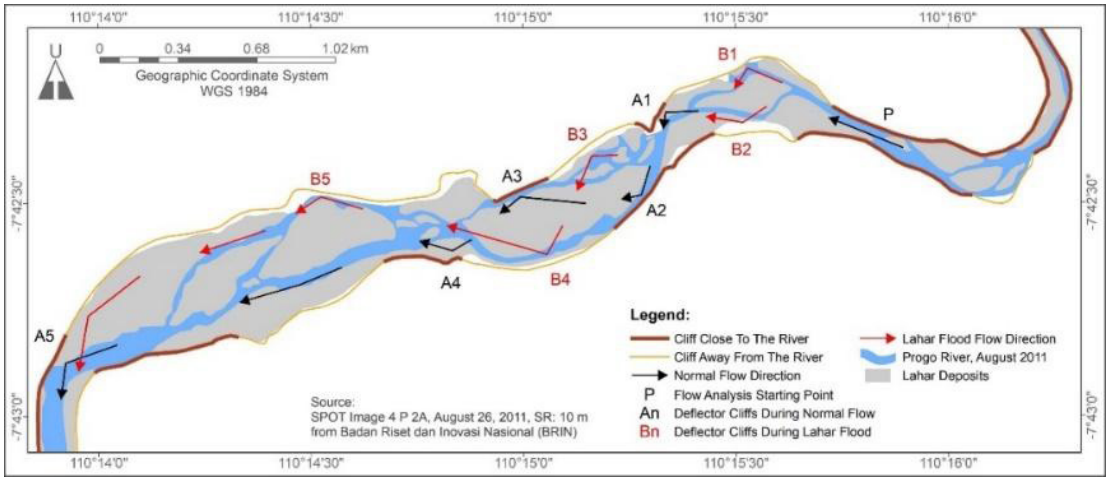

Figure 8. Flow direction during the 2010 lahar event

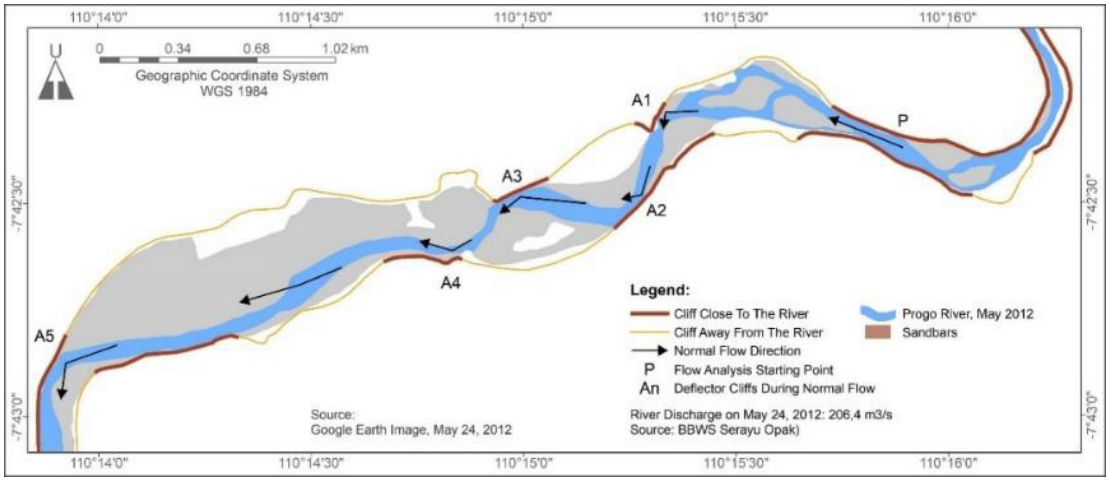

Figure 9. Flow direction after the 2010 Lahar flood

morphology, particularly when the water body is traversed by extreme flow discharges such as lahar floods.

An analysis was carried out to determine riverbank morphology before, during, and after the 2010 lahar flood period. The analysis consisted of a comprehensive observation of the reflection pattern of the flow at the cliffs of the river valley during the three periods, after which the obtained results were compared to examine the changes caused by lahars.

Figure 7 shows morphology of the observed river in its normal condition before the occurrence of lahar flood. As presented in the figure, the analysis was initiated at Point P, a section where the valley cliffs were very close to the river body. At this point, morphology of the stream was in the form of a valley with two widely spaced cliffs. Proceeding Point P, the water body was observed to bend significantly when it encountered a strong and high cliff, denoted as Point A1, which was subsequently referred to as the zone of maximum erosion (Karki et al., 2019). From the observed flow pattern, it can be inferred that the cliff on the opposite side of A1 was away from river body. This area is referred to as river sediment deposition zone (Charlton, 2007). The next river flow (A2-A5) was observed to follow the previous pattern but with a lower

intensity. This was evidenced by the fact that the flow pattern was relatively straight, and the reflection did not get as far as the opposite bank because the strength of the current was not as strong as the initial condition examined. In accordance with the observations made in a previous investigation, the decrease in current strength was caused by the presence of river bends (Charlton, 2007).

The direction of river flow was observed to experience significant changes after the 2010 lahar flood. Figure 8 shows the condition of river on August 26, 2011, eight months after lahar flood. At the period, all parts of the valley in the study area were covered with lahar deposits, showing that at the peak of the flood, lahar flow passed through the entire valley area.

At Points B1 and B2, lahar flow was observed to meander in areas typically distant from the main river body. This variation was more pronounced at Points B3, B4, and B5, where lahar flow showed a significantly bent gradient. Under these conditions, the clear demarcation between the erosion and deposition zones became indistinct.

It is important to emphasize that the flow pattern changed dynamically from the onset of lahar flood to the time the image was recorded and is anticipated to continually evolve as sediment levels decrease. Accordingly, the volume of lahar deposits was found to decrease significantly. This reduction is attributable to two primary factors namely the natural process of sediment being washed away by river over time, and anthropogenic activity, which includes humans extracting lahar materials, such as sand and stone. This extraction is carried out typically through official mining operations with the use of professional equipment and manual collection by residents using simple tools.

Changes were observed in the flow pattern as lahar deposit decreased, and these changes resulted in a reversion to the pre-flood flow pattern. Figure 9 shows the condition of the study area shortly after lahar flood. From the image, it can be seen that the post-flood flow pattern gradually returned to its original state, and although the intensity of changes diminished over time, it did not cease entirely. These river changes were further evidenced by the disappearance and reappearance of riverbanks, narrowing or widening of river channel, and alterations in its course, whether due to natural processes or human activities (Kumar Pal et al., 2017).

Changes in river flow patterns toward the equilibrium line are shown in river morphology maps from 2010 to 2022, excluding 2020 (Figure 10). These maps also emphasized changes in land cover experienced within the valley area. After the 2010 lahar flood, river morphology was found to be in a progressively simpler form. Furthermore, recent land cover conditions showed that human activities had returned to pre-flood levels. This recovery is evident in the presence of paddy fields, mixed fields, and dry fields. It is also important to establish that built-up areas of lahar deposits were found near the river, comprising settlements and buildings for mining activities.

River Curvature

The curvature of the observed river was quantified by the sinuosity ratio (SR). The measurement scheme is shown in Figure 11, where the blue and red lines represent river and valley lengths respectively. This scheme was consistently applied to all data collected during the investigation.

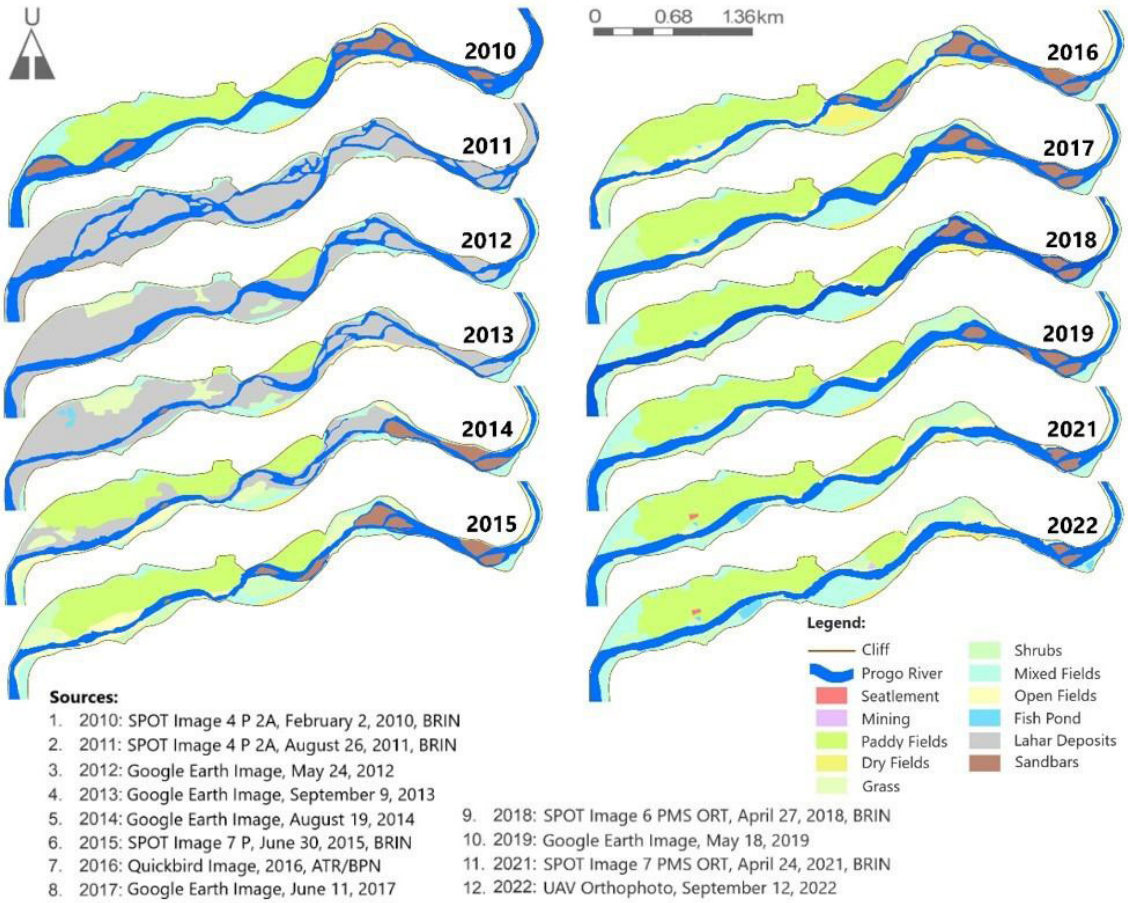

Figure 10. Map of changes in river morphology and land cover in the study area after lahar event from 2010 to 2022

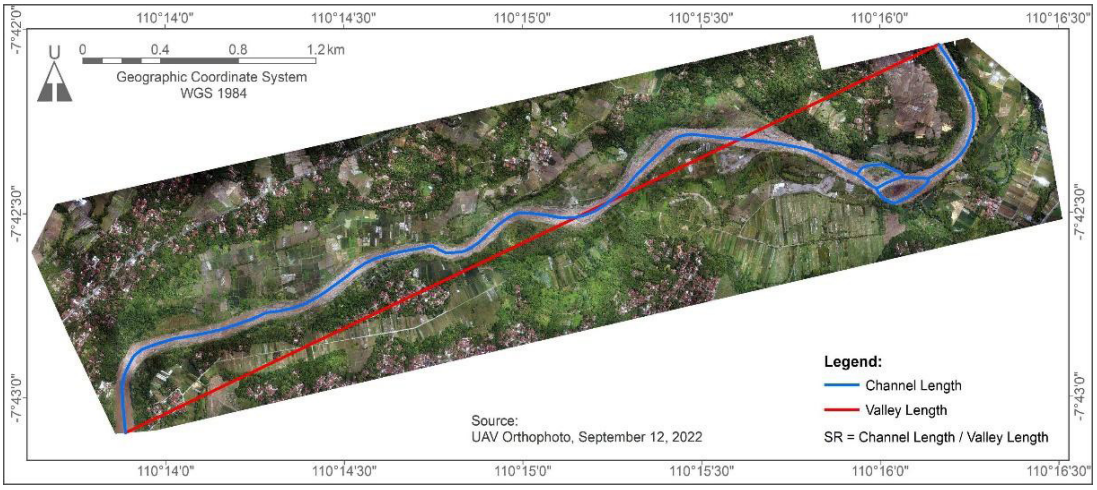

Figure 11.

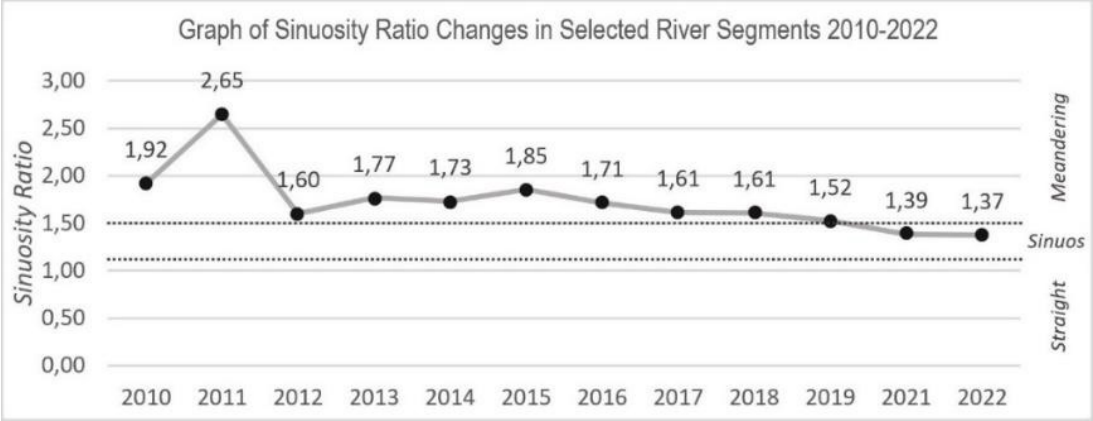

Figure 12. Graph of Sinuosity Ratio Changes in Selected River Segments

The calculation of sinuosity ratio (SR) values was conducted for the observed river over the periods before, during, and after the lahar flood from 2010 to 2022, excluding 2020 (Figure 12). The trend of river curvature was found to fluctuate significantly between 2010 and 2015. Lahar flood at the end of 2010 caused a significant increase in the SR value in 2011. Lahar deposits caused river flow to split and spread throughout the valley in search of a downstream path (Figure 8). Each new flow path is counted as a separate channel in the SR calculation, resulting in a significant increase in the SR value.

The SR value after lahar flood fluctuated for up to four distinct years. In 2012, the SR value was found to decrease significantly from the previous year, reaching a lower level than before lahar flood. This decrease was due to the river's discharge returning to normal and river flow returning to an initial position before the flood. Additionally, the extraction of lahar deposits by human activity and natural river processes, contributed to this reduction. Over the following three years, the SR value exhibited an up-and-down trend, with increases denoting a reduction in the number of separate streams. From 2015 to 2022, the SR value consistently decreased, suggesting that for more than a decade, river had been adjusting towards a more stable pattern. The stability in SR values during this period reflected a balance between erosion and deposition activities (Suresh et al., 2022). It is also important to state that the SR trend in the last two years has been below 1.5, showing that river was no longer meandering but has transitioned to the sinuous category, with fewer and simpler bends.

River Morphology of the 1975 Lahar Flood Period

The dynamics of river morphology changes have occurred not only since the 2010 lahar flood but also in earlier periods. This observation was evidenced by interviews with several residents, which provided information about significant lahar floods in the 20th century. Most sources estimated that these events occurred in the 1970s, with two sources specifically identifying 1975, and one source emphasizing August 1975.

To support the interview information, data was collected to describe river morphology from that period. The primary data includes images of the the PBB Map of Banjarharjo Village from 1972 and the PBB Map of Banjarasri Village from 1980, at a scale of 1:5000, both of which were digitized to examine the river body. The PBB Map of Banjarharjo Village covered the upstream and middle parts of the study area, while the Banjarasri Village map covered the downstream part.

When river morphology from these two PBB maps was overlaid on an aerial photo from 2022, a significant difference in river morphology was observed, as shown in Figure 13. Accordingly, Point A in the 1975 morphology represents a deposition zone that was not drained by water, while, in 2022, it becomes the main flow zone with two sandbars. Points B and C in the 1975 morphology were part of the main flow zone but are now outside river body. However, it is important to establish that Points B and C still show traces of the old river flow pattern. The historical river flow patterns provide critical information and serve as a warning that these areas may become hazard zones when river discharge exceeds normal limits.

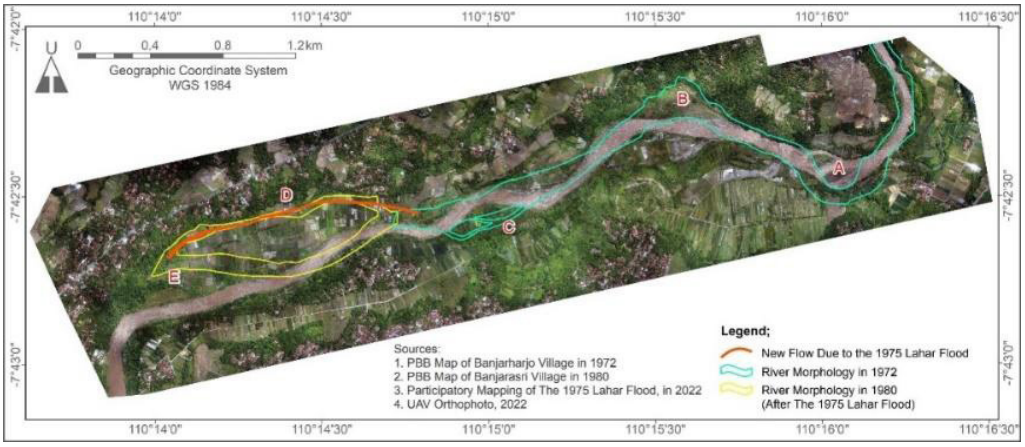

Figure 13. River morphology in the 1975 lahar flood period

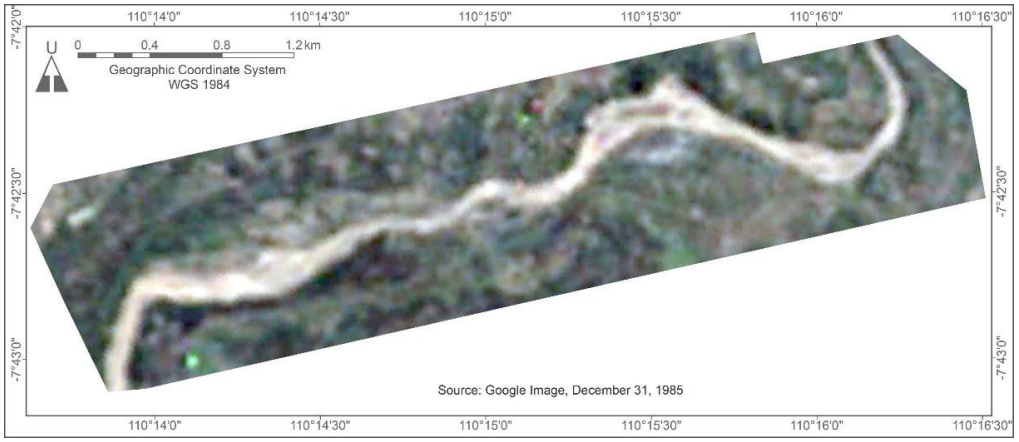

Figure 14. The 1985 Google Earth image

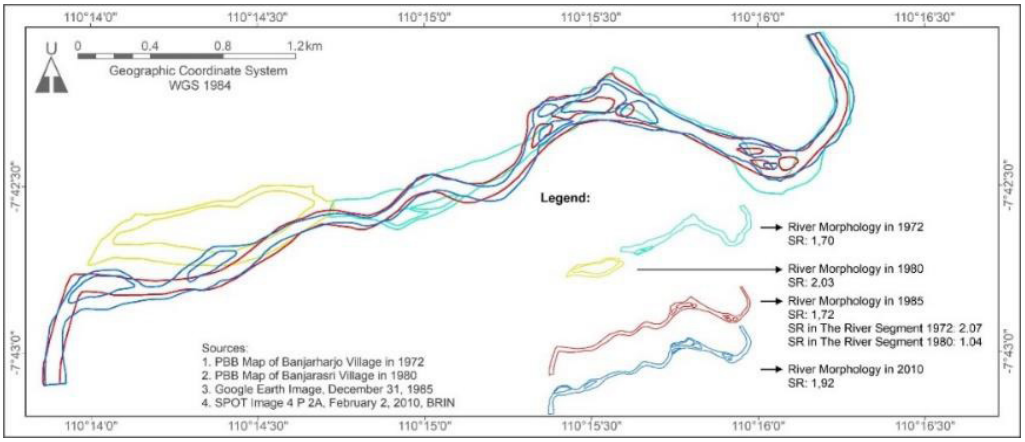

Figure 15. The dynamics of river morphology of the study area from 1972 to 2010

The yellow polygon in Figure 13 shows the river morphology in 1980 and as can be seen, the differences between the previous and current conditions are significant, particularly with the advent of a new flow in the north (Area D), which was formed as a result of the 1975 lahar flood. Additionally, the main flow in the south, which was prominent in 1980, is no longer evident in the current river position and has shifted northward. While map accuracy could contribute to the positional differences, the pattern observed at Point E on the aerial photo confirms that this area was once part of river flow.

To further corroborate the phenomenon of new flows, participatory mapping data was obtained and used during the course of the investigation, which enabled the visualization of Information from residents about new flows. Typically, participatory mapping is a widely recognized method for obtaining effective mapping data from non-experts, hence providing valuable additional data to support the observed changes in river morphology. This form of mapping can be used for coastal and marine ecosystem management (Levine & Feinholz, 2015), urban forest management (Hawthorne et al., 2015), disaster risk management (Bustillos Ardaya et al., 2019), and flood risk management (Cheung et al., 2016), among others. In this study, the mapping was conducted by examining the position of the 1975 lahar flood flow on current UAV aerial photographs. The results, which are indicated by a red line passing through Point D, show a similarity in the location of the new flow with the PBB map, confirming that the entire river valley area is prone to lahar flooding.

Table 2. The development of Sinuosity Ratio in the study area

Years	Channel Length (m)	Valley Length (m)	*SR*	Type
1972	4817,81	2835,69	1,70	*Meandering*
1985 on the 1972 river segment	5856,81	2835,69	2,07	*Meandering*
1980	2808,77	1380,38	2,03	*Meandering*
1985 on the 1980 river segment	1434,02	1380,38	1,04	*Straight*

Source: On-screen digitation and measurements based on image data (2022)

Another datum showing river morphology after the 1975 lahar flood is an image from Google Earth, captured in 1985 (Figure 14). Based on the pattern observed from the two observed lahar floods, the river reverted to its initial position within the next ten years after the occurrence of the disaster. During that period, this river had simpler bends, and new flows formed by Lahar flood had disappeared. The 1985 river morphology is showed by a red line in Figure 15. This figure also shows river morphology from 1972 (before lahar flood), 1980 (after lahar flood), and 2010 (just before the 2010 lahar flood).

Four river morphologies representing different periods were compared in order to show the dynamics (Figure 15). Based on the comparison, significant changes were observed from 1972 to 1985. The middle segment of river appears straighter in 1972 compared to 1985. This difference was further substantiated by the sinuosity ratio (SR) values calculated for the same river segment, as the data for 1972 and 1980 do not cover the entire length of the 1985 segment (Table 2). The SR value for the 1972 river segment was 1.70, while that of the 1985 river segment in the same section increased to 2.07. These changes showed that lahar flood caused river to become more meandering in the upstream and middle segments. Significant changes were also observed to occur in the downstream section from 1980 to 1985. The SR value decreased significantly from 2.03 (showing meandering) in 1980 to 1.04 (showing straight) in 1985. This change is attributable to the flow patterns resulting from the lahar flood, which disappeared within a span of five years, allowing the land to be reused for agriculture. The land use patterns visible in the imagery confirm that agricultural activities were returning to the area.

River morphology in 1985 represents the normal state following the 1975 lahar flood. After the 1975 event, no significant lahar floods were experienced that drastically altered the river morphology until 2010. However, it is important to comprehend that certain changes still occurred (Figure 15). For instance, in 1985, the main channel was observed to be northward, but by 2010, it had shifted southward. Although the main channel in 1985 did not disappear entirely, it left smaller streams separated by sandbars. Sandbars also formed in the upper part of river, adding to the complexity of morphology. This complex morphology was evidenced by the sinuosity ratio (SR) values, which were higher than that of 1985, specifically 1.92 compared to 1.72.

4. Conclusion

In conclusion, based on the examinations carried out during the course of the present investigation, observations were made in favor of the fact that the observed river morphology typically experienced dynamic changes in the years following lahar floods. These changes are usually evidenced by fluctuations in the sinuosity ratio (SR) over the periods spanning multiple lahar flood events. Accordingly, it was also observed that the dynamic nature of the river morphology served as a warning of potential future hazards. This prompted the need for effective spatial planning to mitigate risks associated with river dynamics and lahar floods.

In this study, temporal maps and images played a significant role in analyzing changes in river morphology, and the fluctuations in SR were accurately determined through on-screen digitization and measurements using temporal images. The study shows that quantitative spatial and temporal analysis is more efficient and economical compared to traditional field survey methods. However, it is important to state that these methods provide robust evidence for studying the dynamics of river morphology over time.

Acknowledgment

The authors would like to express gratitude to Sekolah Pascasarjana Universitas Gadjah Mada for permitting the investigation to be conducted in the study area. Furthermore, the investigators would also love to extend gratitude to Pusat Pembinaan, Pendidikan dan Pelatihan Perencana (Pusbindiklatren) Kementerian PPN/ Bappenas and Kementerian Agraria dan Tata Ruang/ BPN for funding this study.

References

Asmara, R. A., Prasetyo, A., Stevani, S., & Hapsari, R. I. (2021). Prediksi Banjir Lahar Dingin pada Lereng Merapi menggunakan Data Curah Hujan dari Satelit. *Jurnal Informatika Polinema*, *7*(2), 35–42. https://doi.org/10.33795/JIP.V7I2.494

Bustillos Ardaya, A., Evers, M., & Ribbe, L. (2019). Participatory approaches for disaster risk governance? Exploring participatory mechanisms and mapping to close the communication gap between population living in flood risk areas and authorities in Nova Friburgo Municipality, RJ, Brazil. *Land Use Policy*, *88*, 104103. https://doi.org/10.1016/J.LANDUSEPOL.2019.104103

Charlton, R. (2007). Fundamentals of fluvial geomorphology. In *Fundamentals of Fluvial Geomorphology*. Taylor and Francis. https://doi.org/10.4324/9780203371084

Cheung, W., Houston, D., Schubert, J. E., Basolo, V., Feldman, D., Matthew, R., Sanders, B. F., Karlin, B., Goodrich, K. A., Contreras, S. L., & Luke, A. (2016). Integrating resident digital sketch maps with expert knowledge to assess spatial knowledge of flood risk: A case study of participatory mapping in Newport Beach, California. *Applied Geography*, *74*, 56–64. https://doi.org/10.1016/j.apgeog.2016.07.006

De Bélizal, E., Lavigne, F., Hadmoko, D. S., Degeai, J. P., Dipayana, G. A., Mutaqin, B. W., Marfai, M. A., Coquet, M., Mauff, B. Le, Robin, A. K., Vidal, C., Cholik, N., & Aisyah, N. (2013). Rain-triggered lahars following the 2010 eruption of Merapi volcano, Indonesia: A major risk. *Journal of Volcanology and Geothermal Research*, *261*, 330–347. https://doi.org/10.1016/J.JVOLGEORES.2013.01.010

Encyclopedia of volcanoes. (2000). *Encyclopedia of Volcanoes*. https://doi.org/10.1063/1.1325206

Gudmundsson, M. T. (2015). Hazards from Lahars and Jökulhlaups. *The Encyclopedia of Volcanoes*, 971–984. https://doi.org/10.1016/B978-0-12-385938-9.00056-0

Hadmoko, D. S., de Belizal, E., Mutaqin, B. W., Dipayana, G. A., Marfai, M. A., Lavigne, F., Sartohadi, J., Worosuprojo, S., Starheim, C. C. A., & Gomez, C. (2018). Post-eruptive lahars at Kali Putih following the 2010 eruption of Merapi volcano, Indonesia: occurrences and impacts. *Natural Hazards*, *94*(1), 419–444. https://doi.org/10.1007/S11069-018-3396-7

Hasan, G. M. J., Jabir, A. Al, & Anam, M. M. (2022). Monitoring bank-line movements of the rivers flowing across the Sundarbans using remote sensing and GIS techniques. *Regional Studies in Marine Science*, *56*, 102679. https://doi.org/10.1016/J.RSMA.2022.102679

Hawthorne, T. L., Elmore, V., Strong, A., Bennett-Martin, P., Finnie, J., Parkman, J., Harris, T., Singh, J., Edwards, L., & Reed, J. (2015). Mapping non-native invasive species and accessibility in an urban forest: A case study of participatory mapping and citizen science in Atlanta, Georgia. *Applied Geography*, *56*, 187–198. https://doi.org/10.1016/J.APGEOG.2014.10.005

Islami, M. (2014). Analisis Perubahan Meander Saluran Tanah Akibat Variasi Debit (Uji Model Laboratorium). *Jurnal Teknik Sipil Dan Lingkungan*, *2*(3), 314–319.

Karki, S., Nakagawa, H., Kawaike, K., & member of JSCE, S. (2019). MEANDERING CHANNELS RESPONSE TO A SERIES OF PERMEABLE AND IMPERMEABLE STRUCTURES UNDER DIFFERENT SINUOSITY. *Journal of Japan Society of Civil Engineers, Ser. B1 (Hydraulic Engineering)*, *75*(2), I_1021-I_1026. https://doi.org/10.2208/JSCEJHE.75.2_I_1021

Kumar Pal, P., Rahman, A., & Anika Yunus, D. (2017). Analysis on River Bank Erosion-Accretion and Bar Dynamics Using Multi-Temporal Satellite Images. *American Journal of Water Resources*, *5*(4), 132–141. https://doi.org/10.12691/ajwr-5-4-6

Levine, A. S., & Feinholz, C. L. (2015). Participatory GIS to inform coral reef ecosystem management: Mapping human coastal and ocean uses in Hawaii. *Applied Geography*, *59*, 60–69. https://doi.org/10.1016/J.APGEOG.2014.12.004

Mead, S., Magill, C., & Hilton, J. (2016). Rain-triggered lahar susceptibility using a shallow landslide and surface erosion model. *Geomorphology*, *273*, 168–177. https://doi.org/10.1016/J.GEOMORPH.2016.08.022

Minami, Y., Ohba, T., Hayashi, S., Saito-Kokubu, Y., & Kataoka, K. S. (2019). Lahar record during the last 2500 years, Chokai Volcano, northeast Japan: Flow behavior, sourced volcanic activity, and hazard implications. *Journal of Volcanology and Geothermal Research*, *387*. https://doi.org/10.1016/J.JVOLGEORES.2019.106661/LAHAR_RECORD_DURING_THE_LAST_2500_YEARS_CHOKAI_VOLCANO_NORTHEAST_JAPAN_FLOW_BEHAVIOR_SOURCED_VOLCANIC_ACTIVITY_AND_HAZARD_IMPLICATIONS.PDF

Pistolesi, M., Cioni, R., Rosi, M., & Aguilera, E. (2014). Lahar hazard assessment in the southern drainage system of Cotopaxi volcano, Ecuador: Results from multiscale lahar simulations. *Geomorphology*, *207*, 51–63. https://doi.org/10.1016/J.GEOMORPH.2013.10.026

Saepuloh, A., Urai, M., Aisyah, N., Sunarta, Widiwijayanti, C., Subandriyo, & Jousset, P. (2013). Interpretation of ground surface changes prior to the 2010 large eruption of Merapi volcano using ALOS/PALSAR, ASTER TIR and gas emission data. *Journal of Volcanology and Geothermal Research*, *261*, 130–143. https://doi.org/10.1016/J.JVOLGEORES.2013.05.001

Saputra, T. M. (2013). EVALUATION OF DISASTER MITIGATION SYSTEM AGAINST LAHAR FLOW OF PUTIH RIVER, MT. MERAPI AREA. *Journal of the Civil Engineering Forum*, *22*(3). https://doi.org/10.22146/JCEF.18904

Sarif, M. N., Siddiqui, L., Islam, M. S., Parveen, N., & Saha, M. (2021). Evolution of river course and morphometric features of the River Ganga: A case study of up and downstream of Farakka Barrage. *International Soil and Water Conservation Research*, *9*(4), 578–590. https://doi.org/10.1016/J.ISWCR.2021.01.006/EVOLUTION_OF_RIVER_COURSE_AND_MORPHOMETRIC_FEATURES_OF_THE_RIVER_GANGA_A_CASE_STUDY_OF_UP_AND_DOWNSTREAM_OF_FARAKKA_BARRAGE.PDF

Suresh, A., Chanda, A., Rahaman, Z. A., Kafy, A. Al, Rahaman, S. N., Hossain, M. I., Rahman, M. T., & Yadav, G. (2022). A geospatial approach in modelling the morphometric characteristics and course of Brahmaputra river using sinuosity index. *Environmental and Sustainability Indicators*, *15*, 100196. https://doi.org/10.1016/J.INDIC.2022.100196

Thouret, J. C., Antoine, S., Magill, C., & Ollier, C. (2020). Lahars and debris flows: Characteristics and impacts. In *Earth-Science Reviews* (Vol. 201). Elsevier B.V. https://doi.org/10.1016/j.earscirev.2019.103003

Van Zuidam, R. A. (1986). Aerial photo-interpretation in terrain analysis and geomorphologic mapping. *Aerial Photo-Interpretation in Terrain Analysis and Geomorphologic Mapping*. https://doi.org/10.2307/634926